The Effect of Al and Cu Electrode Configurations on the Thermoelectric Performance of PVA/glycerin/H3PO4-Based Ionic Thermoelectric Cells

Fadli Robiandi[1,2]*, Dian Mart Shoodiqin[1], & Menasita Mayantasari[1]
[1]Physics Study Program, Institut Teknologi Kalimantan, Indonesia
[2]Electrochemistry Research Center, Institut Teknologi Kalimantan, Indonesia
*Corresponding Author: fadlirobiandi@lecturer.itk.ac.id

Received: 1st September 2025; **Accepted**: 17th November 2025; **Published**: 4th December 2025
DOI: https://dx.doi.org/10.29303/jpft.v11i2.10141

Abstract *– Ionic thermoelectric (i-TE) materials have the potential to be applied to devices for converting low-temperature heat energy into electricity. In this study, an I-TE cell made of PVA/glycerin/H_3PO_4 was synthesized using Al and Cu electrodes. The general objective of this study is to investigate how symmetrical electrode configurations (Al-Al, Cu-Cu) and asymmetrical configurations (Al-Cu) affect the thermoelectric performance of PVA/glycerin/H_3PO_4 polymer electrolyte cells, including potential difference, Seebeck coefficient, and power factor. The results of this study show that the PVA/glycerin/H_3PO_4 sample with asymmetric electrodes produces a higher potential difference than the sample with symmetric electrodes. The highest potential difference in the sample with asymmetric electrodes is 0.97 V. Meanwhile, the highest potential difference produced by the sample with symmetrical Al electrodes was 0.15 V. However, the highest increase in potential difference with respect to temperature gradient was observed in the PVA/glycerin sample with symmetrical Al electrodes. This was based on the Seebeck coefficient value produced by the sample, which was 16 mV/K. This is followed by the sample with an asymmetric electrode, and the lowest is the sample with a symmetric Cu electrode. The power factor of the sample increases with increasing temperature and follows the pattern of increasing ionic conductivity. In addition, the power factor is also influenced by the Seebeck coefficient value of the sample. In this study, samples with symmetrical Al electrodes showed the highest PF values, with a maximum value at a temperature of 65 °C. These findings indicate that polymer electrolyte cells based on PVA/glycerin/H_3PO_4 with Al and Cu electrodes have the potential for use in i-TE devices to convert low-quality thermal energy into electricity.*

Keywords*: ionic thermoelectric; PVA; Al-Cu electrode; Seebeck Coefficient; Power Factor.*

INTRODUCTION

The abundant availability of low-temperature thermal energy (<100°C) – from solar radiation to industrial waste heat – represents a vast and underutilized source of renewable energy. Harnessing this thermal energy presents a significant challenge yet also a major opportunity for energy sustainability. One promising approach is the direct conversion of thermal energy into electrical energy via the thermoelectric (TE) effect. Devices that apply this effect are thermoelectric generators (TEG). TEG are composed of TE material cells. Conventional TE materials based on semiconductors (Shi et al., 2020) often have high material costs (Zheng et al., 2021), are relatively difficult to produce, and contain toxic elements (Liu et al., 2021). This limits their widespread application. In addition, these materials work more optimally at high temperatures (>100ºC) (T. Y. Kim et al., 2016; Shi et al., 2020). These shortcomings have prompted researchers to explore alternative TE materials that are more environmentally friendly, inexpensive, and efficient, especially for low-temperature heat-to-electricity conversion applications.

As the demand for renewable energy sources increases, the conversion of low-grade thermal energy becomes increasingly relevant. Ionic thermoelectric (i-TE) materials have the potential to be an innovative solution to this need. The

mechanism of electrical voltage generation in i-TE materials differs from that of semiconductor TE materials. i-TE materials utilize the movement of ions in electrolytes to generate electrical voltage (Han et al., 2020). i-TE materials exhibit a Seebeck coefficient that is significantly higher than conventional semiconductors at low temperatures (Liu et al., 2021). One type of i-TE material is polymer electrolyte. Polyvinyl alcohol (PVA) combined with glycerin and H_3PO_4 is an ideal candidate as a polymer electrolyte to be applied in i-TE. This material not only has good mechanical stability (Zhao et al., 2020) but also tunable ionic conductivity (Xue et al., 2015). Additionally, it is easy to shape as it is soluble in water. However, the performance of i-TE devices is significantly influenced by the interface interaction between the electrodes and the electrolyte, which affects ion movement and conversion efficiency.

Previous studies have explored PVA-based i-TEs, significant knowledge gaps remain. Early work by Mostafa et al. achieved 9.26 mV/K in salt-free PVA hydrogels (Yossef et al., 2024), while Suk Lae Kim et al, reported 1-1.5 mV/K in PVA solid electrolytes with NaOH and H_3PO_4 (S. L. Kim et al., 2018). While extensive literature exists on optimizing the bulk properties of PVA-based electrolytes for i-TE performance, a critical knowledge void persists regarding the electrode-electrolyte interfacial dynamics. No systematic comparative study has been reported to date quantifying how common metallic electrode configurations (e.g., Al-Al, Cu-Cu vs. Al-Cu) modulate the Power Factor and Seebeck coefficient in the PVA/glycerin/H_3PO_4 system.

The primary objective is to quantitatively compare and contrast the potential difference, Seebeck coefficient, and Power Factor for symmetric (Al-Al, Cu-Cu) and asymmetric (Al-Cu) PVA/glycerin/H_3PO_4 ionic thermoelectric cells. This study quantitatively evaluate three key performance metrics: different potential, Seebeck coefficient, and power factor. The results of this study can contribute to understanding how electrode combinations and their interaction with polymer electrolytes affect i-TE performance and energy conversion efficiency. This opens the way for designing more effective low-grade thermal power conversion devices based on i-TE materials.

RESEARCH METHODS

a) Raw Materials

The polymer electrolyte was synthesized using polyvinyl alcohol (PVA) as the polymer matrix and glycerin as the plasticizer. The electrolyte solution consisted of 85% wt phosphoric acid (H_3PO_4) as the ionic dopant. Distilled water served as the solvent for polymer dissolution. All chemicals were reagent-grade and procured from commercial suppliers.

b) Gel Electrolyte Synthesis

The PVA/glycerin electrolyte was prepared through a three-step process: PVA gel formation, glycerin and H_3PO_4 incorporation, and solvent casting. First, a homogeneous PVA gel was prepared by dissolving 2 g of PVA powder in 40 g of distilled water under constant stirring. Subsequently, 4 g of glycerin and 6 g of H_3PO_4 as ionic source were incorporated into the PVA gel with continuous mixing until complete homogenization. The resulting electrolyte solution was then cast into petri dishes and dried at 35°C for 20 hours in a temperature-controlled oven.

c) Ionic Conductivity Measurement

The ionic conductivity was measured using the experimental setup shown in Figure 1. PVA/Glycerin polymer electrolyte samples were loaded into cylindrical plastic molds with 4.5 mm inner diameter. The gel electrolyte was uniformly compressed between two copper plate electrodes, ensuring complete filling of the measurement cell without air gaps. These copper plates functioned as electrodes during the conductivity measurements.

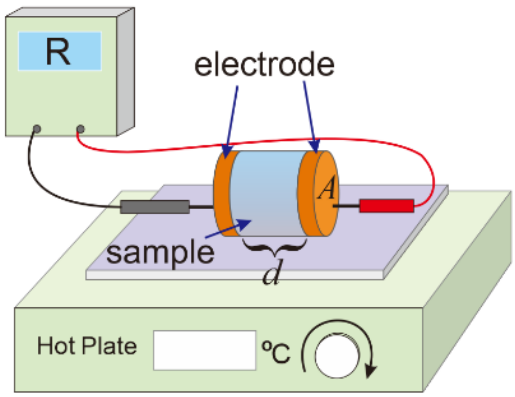

Figure 1. Ionic conductivity mesurement setup

Electrical conductivity (σ) could be calculated using equation 1.

$$\sigma = \frac{d}{R_B A} \qquad (1)$$

Based on equation 1, d is the length of the sample in the tube (m). R_B is the electrical resistance of the sample (ohm). A is the cross-sectional area of the sample in the plastic tube (m^2).

d) Potential Difference Measurement

The measurement configuration for characterizing the output voltage is shown in Figure 2. The polymer electrolyte sample was poured into a plastic tube with dimensions of 4.5 mm inner diameter × 3 mm length. The tube was sealed with electrodes made of aluminum and copper foil. The electrode configuration is shown in Table 1. Voltage measurements were performed over a temperature range of 30–65°C (with 5°C intervals) using the following instruments: a PID-controlled digital hot plate for precise heating, a Sanwa CD800a digital multimeter, and a type-K thermocouple with digital readout for temperature monitoring (Robiandi et al., 2024).

Table 1. Electrode Configuration

No.	Sample	Electrode configuration
1.	Configuration A	Al on the hot side and Cu on the cold side of the sample.
2.	Configuration B	Cu on the hot side and Al on the cold side of the sample.
3.	Configuration C	The hot and cold side of the sample use Al.
4.	Configuration D	The hot and cold side of the sample use Cu.

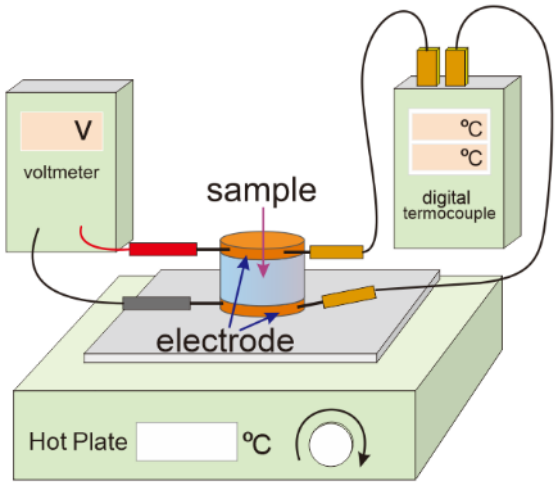

Figure 2. Differences in the potential measurement setup

e) Analysis of Seebeck Coefficient and Power Factor and Activation Energy

The Seebeck coefficient could be calculated from the equation 2.

$$S = \frac{\Delta V}{\Delta T} \qquad (2)$$

where: ΔV is voltage difference (V). ΔT is temperature gradient (K).

In this study, several variations of data were used, so that the Seebeck coefficient was determined from the linear regression slope of the ΔV versus ΔT plot according to equation 3:

$$S = \frac{n\sum_{i=1}^{n} x_i y_i - \sum_{i=1}^{n} x_i \sum_{i=1}^{n} y_i}{n\sum_{i=1}^{n} x_i^2 - (\sum_{i=1}^{n} x_i)^2} \quad (3)$$

S is Seebeck coefficient (V/K), n represents measurement points, x_i is temperature gradients (ΔT), and y_i corresponds to measured potential difference (ΔV).

The power factor (PF) was evaluated using equation 4:

$$PF = \sigma S^2 \quad (4)$$

where: σ is ionic conductivity (S m^{-1}). (Li et al., 2022).

The activation energy (E_a) was determined from the slope (b) of the Arrhenius conductivity plot according to equation 5:

$$b = -E_a/k_B \quad (5)$$

k_B represents the Boltzmann constant. This relationship derives from the Arrhenius conductivity equation 6 (Johannes et al., 2022):

$$\sigma_T = \sigma_0 \, exp(-E_a/(k_B\, T)) \quad (6)$$

σ_T is ionic conductivity at temperature (mS/m), σ_0 is pre-exponential factor (mS/m), T is temperature (K)

RESULTS AND DISCUSSION

Result

a) Gel Electrolyte

The electrolyte polymer synthesized from PVA, glycerin, and H_3PO_4 solution in this study is shown in Figure 3. In this study, the PVA-glycerin electrolyte polymer is transparent and elastic.

Figure 3. PVA/glycerine/H_3PO_4 polymer electrolyte

b) Potential Difference and Seebeck Coefficient

Based on the results of this study, the potential difference of the PVA/glycerin polymer electrolyte exhibits a positive correlation with increasing heating temperature or hot-side temperature of sample. The asymmetric electrode configurations (A and B) demonstrate significantly enhanced voltage output compared to their symmetric counterparts (C and D). Configuration B achieves optimal performance, reaching a maximum potential difference of 0.97 V at 65°C, while configuration D shows minimal response (0.1 V at 30°C). The relationship between potential difference and heating temperature is shown in Figure 4.

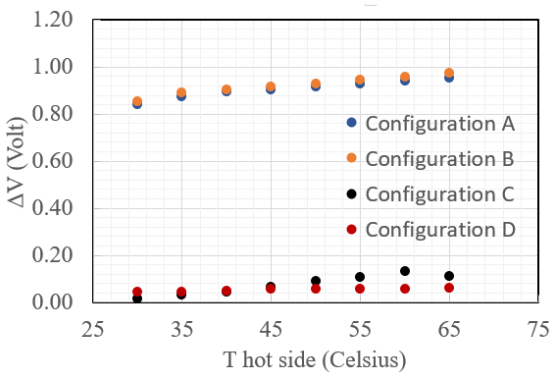

Figure 4. Potential difference at varying heating temperature

The results of measuring the potential difference against the temperature difference are shown in Figure 5.

Figure 5 demonstrated a positive correlation between the temperature gradient (ΔT) and the generated potential difference (ΔV) across all sample configurations. The

asymmetric electrode configurations showed significantly better thermoelectric performance compared to symmetric configurations, with configuration B achieving the maximum potential difference of 0.97 V at temperature gradient = 7.71 K. In contrast, configuration D shows minimal response, generating only 0.06 V at a comparable temperature gradient of 7.51 K. This 16-fold enhancement in output voltage highlights the critical role of electrode asymmetry in optimizing ionic thermoelectric performance.

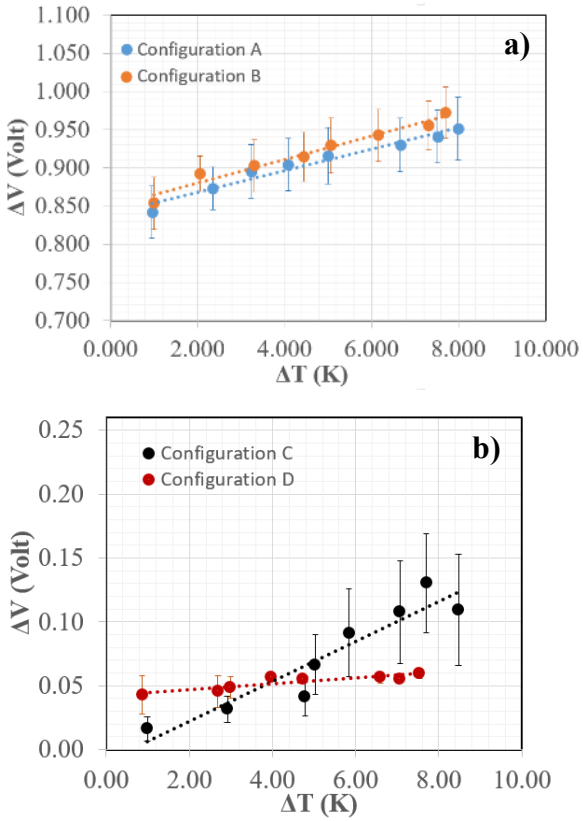

Figure 5. Potential differences at varying temperature difference. a) asymmetry electrode configuration. b) symmetry electrode configuration

The asymmetric electrode configurations (A and B) generated a significantly higher potential difference than those with symmetrical electrodes (C and D). This enhancement is primarily due to a dominant galvanic mechanism. The inherent electrochemical potential difference between the metals, where the more electronegative Al acts as the anode and Cu acts as the cathode, drives a competing redox process. To confirm the galvanic contribution, refers to standard cell potential E^{o}_{cell} calculation (equation 7) for reaction Al oxidation coupled with the reduction of H^{+} ions from the H_3PO_4 electrolyte. Using standard reduction potentials ($H^{+}|H_2$ = 0.00V and $Al^{3+}|Al$ = -1.66 V). the resulting standard potential is:

$$E^{0}_{cell} = E^{0}_{reduction}\,(H^{+}|\,H_2) - E^{0}_{oxidation}\,(Al^{3+}|\,Al) = 0.00\,V - (-1.66\,V) = +1.66V \quad (7)$$

This calculated standard potential of 1.66 V significantly exceeds the maximum observed ΔV of 0.97 V achieved by Configuration B. This comparison confirms that galvanic driving force is thermodynamically present in the asymmetric cells, dominating the total potential output. The fact that the observed voltage is lower than the theoretical 1.66 V is attributed to the kinetically limited redox reactions and the high internal resistance of the polymer electrolyte. This disparity underscores that the output in asymmetric cells is primarily dictated by the difference in metal electrochemical potential and not solely the thermal gradient.

Symmetrical electrode configuration (Al-Al or Cu-Cu) is crucial because in this configuration, the effect of galvanic potential differences between electrodes can be eliminated. Thus, in a symmetrical configuration, the mechanism of potential difference generation due to temperature gradient in the PVA/glycerin/H_3PO_4 cell is only caused by the soret effect.

The Seebeck coefficients were determined from the linear regression slopes

of the ΔV-ΔT curves in Figure 5. As summarized in Table 2, configuration C showed the highest Seebeck coefficient (16.2 mV/K), evidenced by its steepest slope in Figure 5. Interestingly, despite this superior thermoelectric response, configuration C generated lower potential differences than configurations A and B.

Table 2. Seebeck Coefficient

No.	Sample	Seebeck Coefficient (mV/K)
1.	Configuration A	14,5
2.	Configuration B	15,2
3.	Configuration C	16,2
4.	Configuration D	2,3

c) Ionic Conductivity

The results of ionic conductivity measurements of PVA-Glycerine samples ware shown in Figure 6.

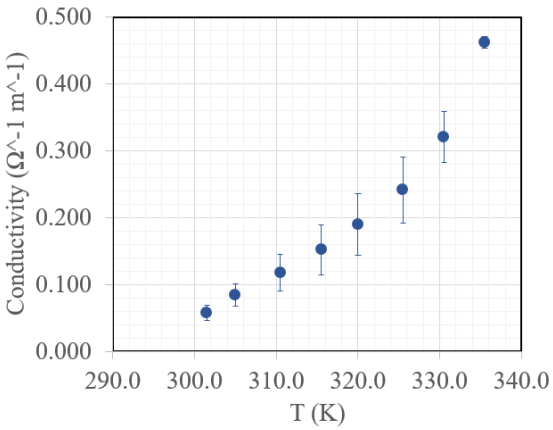

Figure 6. Ionic conductivity at varying temperature.

Figure 6 illustrated the temperature-dependent ionic conductivity of the PVA/glycerin/H_3PO_4 electrolyte, showed a nonlinear increase with rising temperature. The system achieved maximum ionic conductivity (0.46 $\Omega^{-1}m^{-1}$) at 65°C. This thermally activated behavior follows Arrhenius kinetics, as evidenced by the linear relationship in the Arrhenius plot (Figure 7).

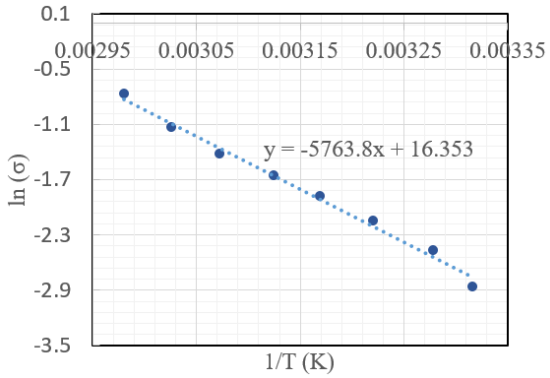

Figure 7. Arrhenius Plot of ionic conductivity.

d) Power Factor

Figure 8 presented the temperature-dependent power factor for all sample configurations, with each configuration reaching its maximum value at the highest test temperature (335.5 K). Configuration C demonstrated highest power factor of 1.34 × 10^{-4} $Wm^{-1}K^{-2}$.

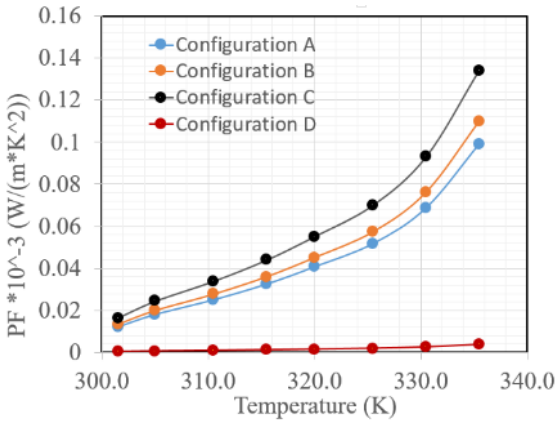

Figure 8. Power factor at varying temperature.

Discussion

An increase in the temperature gradient enhanced the potential difference (voltage) between the cold and hot sides of the sample. This phenomenon arises due to the polarization of ions within the material. A higher temperature gradient promotes greater separation of cations and anions, leading to increased charge polarization. The linear relationship between the potential difference and the temperature gradient was illustrated in Figure 5.

The potential difference generated under a temperature gradient can be attributed to the Soret effect, which describes the thermodiffusion of ions in a polymer electrolyte. When a temperature gradient is applied, cations and anions migrate toward opposite ends of the PVA-Glycerine matrix, leading to charge polarization. Specifically, anions accumulate in the hotter side, while cations concentrate in the colder side (Cheng & Ouyang, 2022; Muddasar et al., 2024). This ionic redistribution establishes the observed voltage across the sample.

Experimental results showed that symmetrical electrode (configurations C and D) had negative potential values at the cold-side electrode and positive values at the hot-side electrode. In the PVA/glycerin/H_3PO_4 polymer matrix, the H_3PO_4 electrolyte dissociated into anions ($H_2PO_4^-$, HPO_4^{2-}, PO_4^{3-}) and cations (H^+). Under the applied temperature gradient, H^+ ions migrated toward the cold side, while $H_2PO_4^-$ anions diffused toward the hot side. This caused an accumulation of H^+ ions on the cold side, due to the attraction electrons from the adjacent metal electrode, resulting in a net negative charge on the cold side electrode. Conversely, the depletion of H^+ ions on the hot side left the corresponding electrode positively charged. This mechanism is illustrated in Figure 9.

Samples with configuration D exhibited low voltage outputs, likely due to the low electrochemical reactivity of copper. Unlike aluminum, copper showed minimal Faradaic activity in the PVA/Glycerin/H_3PO_4 matrix, primarily because of its inertness in acidic environments. Two factors that could contribute to this behavior: Limited H^+ adsorption and anion repulsion. In Limited H^+ Adsorption, Cu had low affinity for proton (H^+) adsorption, preventing significant H^+ accumulation on the cold side. In contrast, Al readily formed surface Al-OH groups via its native oxide layer, facilitating H^+ binding. In Anion Repulsion, the Cu surface developed a slight positive charge in aqueous H_3PO_4, electrostatically repelling $H_2PO_4^-$ anions. This repulsion further inhibited anion accumulation near the electrode, reducing charge asymmetry. Consequently, the combined effected of sluggish H^+ adsorption and $H_2PO_4^-$ repulsion restrict polarization efficiency in Cu-based systems, resulting in diminished thermoelectric performance compared to Al electrodes.

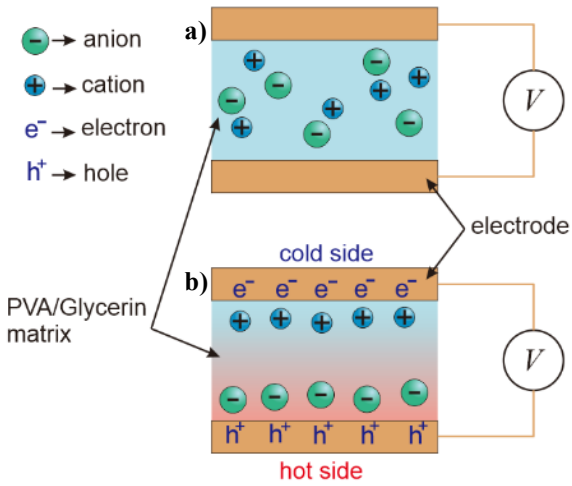

Figure 9. soret effect mechanism in cell with symmetry electrode. a) sample before heating, b) heated sample condition

Samples with asymmetrical electrodes (configurations A and B) generated a significantly higher potential difference than those with symmetrical electrodes (configurations C and D). This enhancement appeared from a dominant galvanic mechanism, which subtituted the Soret effect in these systems. Due to the inherent electrochemical potential difference between the metals, the more electronegative Al electrode consistently exhibits a negative potential, while the Cu electrode maintains a positive potential. In the PVA/glycerin/H_3PO_4 polymer

electrolyte, galvanic-driven redox reaction overwhelms the ionic thermoelectric (Soret) effect. The underlying redox process can be represented by reaction equation:

Reaction in Al electrode interface (hot side of the sample) with configuration A, undergoing oxidation:

$$Al \rightarrow Al^{3+} + 3e^{-} \quad (8)$$

Reaction in Cu electrode interface (cold side of the sample) with configuration A, undergoing reduction:

$$2H^{+} + 2e^{-} \rightarrow H_2 \quad (9)$$

At the interface between Cu and the polymer electrolyte, it is possible for H^{+} (protons) reduction occurs rather than reduction of Cu^{2+} because there are no Cu^{2+} ions in the PVA/glycerin sample.

Reaction in Cu electrode interface (hot side of the sample) with configuration B:

$$Cu \rightarrow Cu^{2+} + 2e \quad (10)$$

When Cu is in the hot side of sample, minor oxidation can occur, resulting in Cu^{2+} .

Reaction in Al electrode interface (cold side of the sample) with configuration B is the same as in reaction equation 8. When Al in cold side of sample, The oxidation reaction of Al is slower than on the hot side.

Table 3. Summary comparison electrode configuration

Configuration	Electrode Setup	Dominant ΔV Mechanism	Measured ΔV (Max) [V]	Measured Seebeck (S) [mV/K]	Contribution Rationale
A	Al (Hot) - Cu (Cold)	Galvanic + Soret	0.97	14.5	High ΔV confirms large electrochemical potential difference; lower S shows Soret effect is secondary.
B	Cu (Hot) - Al (Cold)	Galvanic + Soret	0.97	15.2	Highest measured ΔV due to optimized kinetics/charge transfer dynamics in this configuration. Soret effect is secondary.
C	Al (Hot) - Al (Cold)	Pure Soret	0.15	16.2	Low ΔV and highest S confirms pure thermodiffusion; no galvanic contribution.
D	Cu (Hot) - Cu (Cold)	Pure Soret	0.06	2.3	Lowest ΔV and S due to low electrochemical reactivity/inertness of Cu in acidic environment, no galvanic contribution.

The observed difference in potential output between configurations A and B could be attributed to several factors related to electrode reactivity and charge transfer kinetics. In configuration A, Elevated temperature increased Al reactivity in the hot side but H^{+} reduction at the Cu electrode proceeded slowly. This imbalance in reaction rates limited overall charge transfer efficiency. In Configuration B, Mild Cu dissolution occured in the hot side while Al oxidation in the cold side remained slower than in heated Al (Configuration A). The system achieved more balanced reaction kinetics, as the hot Cu electrode showed lower charge transfer resistance facilitating electron exchange. Consequently, Configuration B generated a marginally higher potential difference due to its optimized charge transfer dynamics and balanced redox activity. A comparison of the potential difference generation mechanisms for each electrode configuration is shown in Table 3.

The power factor showed a positive temperature dependence, as shown in Figure 8. This enhancement primarily resulted from increased ionic conductivity at elevated temperatures. Additionally, the power factor demonstrated configuration-dependent behavior due to variations in the Seebeck coefficient across different sample configurations.

Increasing temperature could accelerate the movement of anions and cations in the PVA/glycerin matrix through two main mechanisms: polymer matrix expansion and ion kinetic energy enhancement. increasing thermal energy amplifies the vibrations of the polymer chains, which causes an expansion of the free volume in the gel structure (Gupta et al., 2021; Johannes et al., 2022). This structural modification facilitates easier ion transport through the polymer network. In ion kinetic energy enhancement mechanisms, The additional thermal energy directly increases the kinetic energy of ionic species (Aziz et al., 2018), promoting faster ion diffusion through the electrolyte matrix, and Improved charge transfer efficiency (Shao et al., 2020). These combined effects significantly enhance overall ionic conductivity in the polymer gel system under thermal excitation. The activation energy for ionic transport in the PVA/Glycerin/H_3PO_4 polymer electrolyte system was determined from the slope of the Arrhenius plot (Figure 4), yielding a value of 0.497 eV. This parameter represented the minimum energy barrier that ions must overcome to achieve mobility within the gel polymer matrix.

CONCLUSION

This study demonstrates that asymmetric electrode configurations (Cu-Al) in PVA/glycerin/H_3PO_4-based ionic thermoelectric cells generate significantly higher potential differences than symmetric configurations (Cu-Cu or Al-Al). The enhanced performance arises from dominant galvanic mechanisms in asymmetric cells, while symmetric configurations primarily exhibit Soret effect driven behavior. Electrode asymmetry creates favorable conditions for galvanic charge transfer. Symmetric systems rely solely on ionic thermodiffusion (Soret effect). These results highlight the critical role of electrode selection in optimizing ionic thermoelectric devices, with Cu-Al electrode combination offering superior performance through combined galvanic and thermoelectric effects.

The Seebeck coefficient shows strong temperature dependence, with configuration C achieving the highest value (16.2 mV/K). Configuration B and A demonstrates intermediate performance, while other symmetric arrangements show minimal response. The power factor improvement correlates with both increased ionic conductivity and elevated Seebeck coefficient. Maximum performance occurs at the highest tested temperature gradient.

This work successfully explains the effect of Al-Cu electrode configuration on the Power Factor, Seebeck coefficient, and output voltage of PVA/glycerin/H_3PO_4 ionic thermoelectric cells; however, several critical areas require dedicated future investigation. Future research could focus on dynamic stability testing to evaluate the long-term performance and durability of these cells under continuous thermal cycling conditions. In addition, to move towards practical applications, efforts should be directed towards thermoelectric generator modules. This next phase is crucial and includes methodically investigating series and parallel connection strategies between individual cells to effectively scale the system and maximize the overall voltage and

current output for practical energy harvesting applications.

ACKNOWLEDGMENT

All authors wish to thank the Institute of Research and Community Services (LPPM) of Kalimantan Institut of Technology for the financial support. The authors also acknowledge the kind hands of all members Physics Study Program, Kalimantan Instutut of Technology.

REFERENCES

Cheng, H., & Ouyang, J. (2022). Soret Effect of Ionic Liquid Gels for Thermoelectric Conversion. *The Journal of Physical Chemistry Letters*, *13*(46), 10830–10842. https://doi.org/10.1021/acs.jpclett.2c02645

Gupta, A., Jain, A., & Tripathi, S. K. (2021). Structural, electrical and electrochemical studies of ionic liquid-based polymer gel electrolyte using magnesium salt for supercapacitor application. *Journal of Polymer Research*, *28*(7), 1–11. https://doi.org/10.1007/s10965-021-02597-9

Han, C.-G., Qian, X., Li, Q., Deng, B., Zhu, Y., Han, Z., Zhang, W., Wang, W., Feng, S.-P., Chen, G., & Liu, W. (2020). Giant thermopower of ionic gelatin near room temperature. *Science (New York, N.Y.)*, *368*(6495), 1091–1098. https://doi.org/10.1126/science.aaz5045

Johannes, C., Hartung, M., & Heim, H. P. (2022). Polyurethane-Based Gel Electrolyte for Application in Flexible Electrochromic Devices. *Polymers*, *14*(13). https://doi.org/10.3390/polym14132636

Kim, S. L., Hsu, J.-H., & Yu, C. (2018). Thermoelectric effects in solid-state polyelectrolytes. *Organic Electronics*, *54*, 231–236. https://doi.org/https://doi.org/10.1016/j.orgel.2017.12.021

Kim, T. Y., Negash, A. A., & Cho, G. (2016). Waste heat recovery of a diesel engine using a thermoelectric generator equipped with customized thermoelectric modules. *Energy Conversion and Management*, *124*, 280–286. https://doi.org/https://doi.org/10.1016/j.enconman.2016.07.013

Li, J., Huckleby, A. B., & Zhang, M. (2022). Polymer-based thermoelectric materials: A review of power factor improving strategies. *Journal of Materiomics*, *8*(1), 204–220. https://doi.org/10.1016/j.jmat.2021.03.013

Liu, W., Qian, X., Han, C.-G., Li, Q., & Chen, G. (2021). Ionic thermoelectric materials for near ambient temperature energy harvesting. *Applied Physics Letters*, *118*(2), 20501. https://doi.org/10.1063/5.0032119

Muddasar, M., Menéndez, N., Quero, Á., Nasiri, M. A., Cantarero, A., García-Cañadas, J., Gómez, C. M., Collins, M. N., & Culebras, M. (2024). Highly-efficient sustainable ionic thermoelectric materials using lignin-derived hydrogels. *Advanced Composites and Hybrid Materials*, *7*(2). https://doi.org/10.1007/s42114-024-00863-0

Robiandi, F., Shoodiqin, D. M., & Mayantasari, M. (2024). Performance and Characterization of Seebeck Coefficient and Power Factor in CMC/Glycerin Gel Electrolyte Based Ionic Thermoelectric. *Jurnal Pendidikan Fisika Dan Teknologi*, *10*(2), 230–239. https://doi.org/10.29303/jpft.v10i2.7322

Shi, X.-L., Zou, J., & Chen, Z.-G. (2020). Advanced Thermoelectric Design: From Materials and Structures to Devices. *Chemical Reviews*, *120*(15),

7399–7515. https://doi.org/10.1021/acs.chemrev.0c00026

Xue, Z., He, D., & Xie, X. (2015). Poly(ethylene oxide)-based electrolytes for lithium-ion batteries. *Journal of Materials Chemistry A*, *3*(38), 19218–19253. https://doi.org/10.1039/C5TA03471J

Yossef, M., Baniasadi, H., Kallio, T., Perry, M., & Puttonen, J. (2024). Ionic thermoelectricity of salt-free PVA-hydrogel. *Applied Materials Today*, *38*(May), 102240. https://doi.org/10.1016/j.apmt.2024.102240

Zhao, Q., Stalin, S., Zhao, C.-Z., & Archer, L. A. (2020). Designing solid-state electrolytes for safe, energy-dense batteries. *Nature Reviews Materials*, *5*(3), 229–252. https://doi.org/10.1038/s41578-019-0165-5

Zheng, Y., Slade, T. J., Hu, L., Tan, X. Y., Luo, Y., Luo, Z.-Z., Xu, J., Yan, Q., & Kanatzidis, M. G. (2021). Defect engineering in thermoelectric materials: what have we learned? *Chemical Society Reviews*, *50*(16), 9022–9054. https://doi.org/10.1039/D1CS00347J